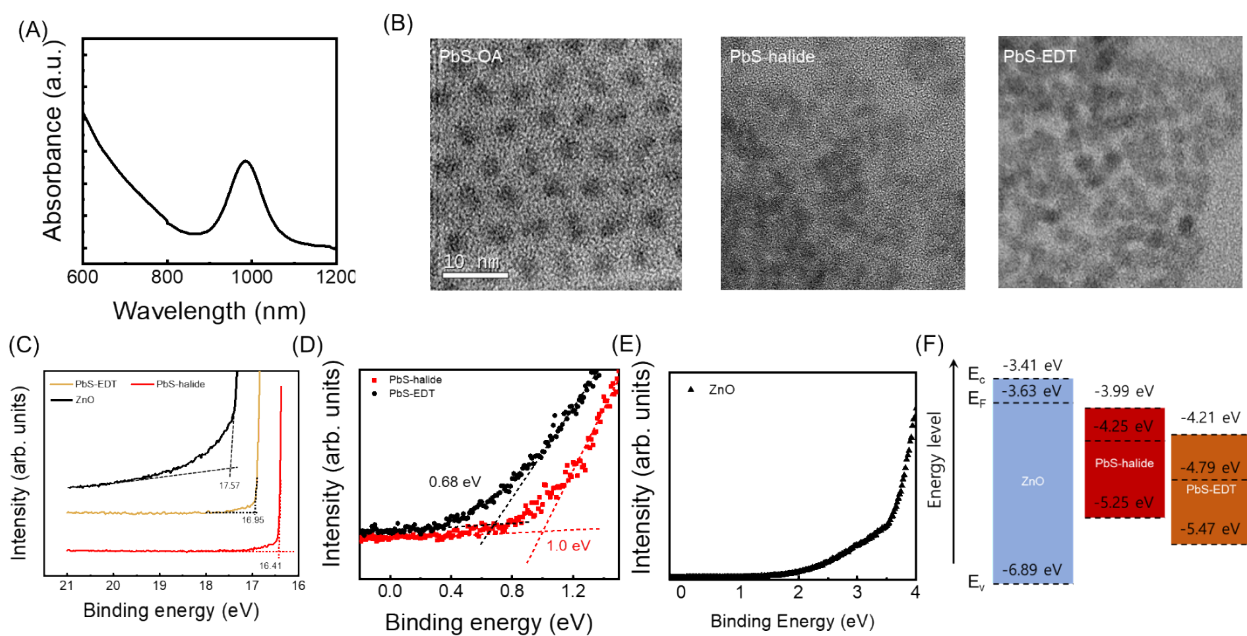


## Supporting Information

**Ultra-sensitive Colloidal Quantum Dot Infrared Photodiode Exceeding 100,000% of External Quantum Efficiency *via* Photomultiplication.**

*Byung Ku Jung, Taesung Park, Young Kyun Choi, Yong Min Lee, Tae Hyuk Kim, Bogyom Seo, Seongkeun Oh, Jae Won Shim, Yu-hwa Lo, Tse Nga Ng, Soong Ju Oh\**



**Figure S1.** (A) UV-vis spectra of PbS CQDs. (B) TEM image of PbS-OA, PbS-halide, and PbS-EDT. UPS spectra of the (C) cut-off and (D, E) onset region for ZnO, PbS-OA, PbS-halide, and PbS-EDT. (F) The total band diagram of ZnO, PbS-OA, PbS-halide, and PbS-EDT.

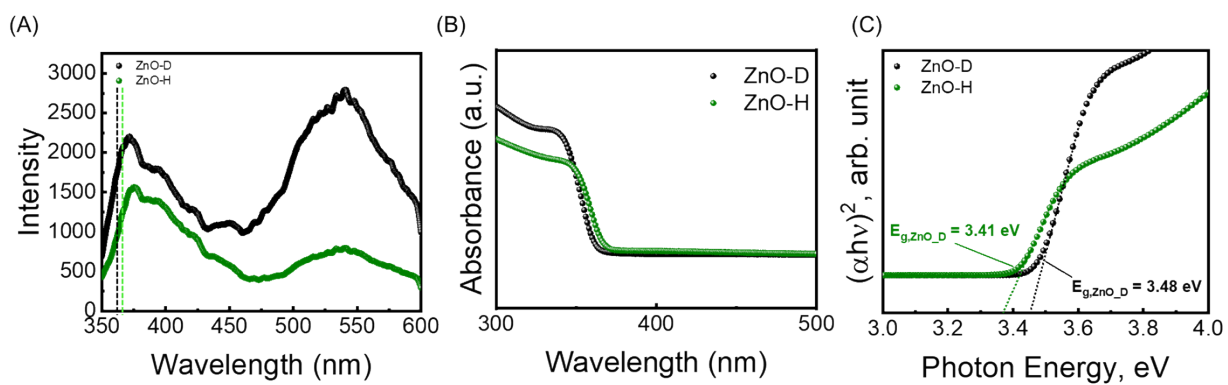


**Figure S2.** (A) PL and (B) UV-vis spectra of ZnO-pristine and ZnO-Hydrated. (C) Tauc plot calculated from the UV-vis spectra.

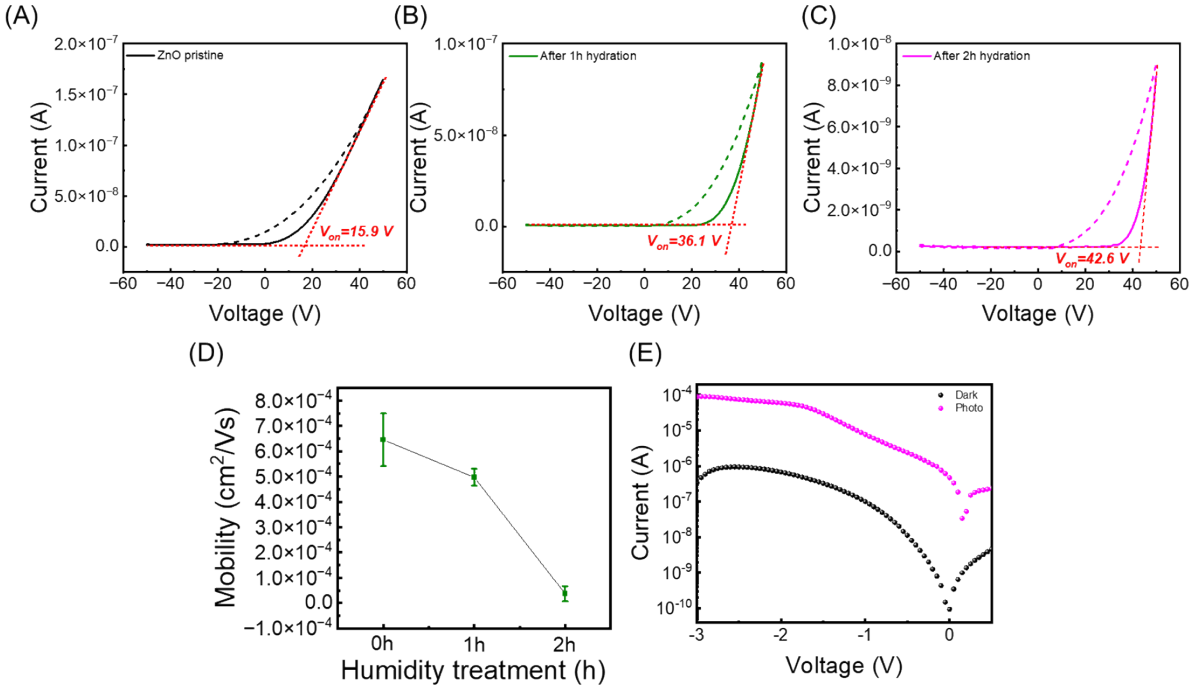
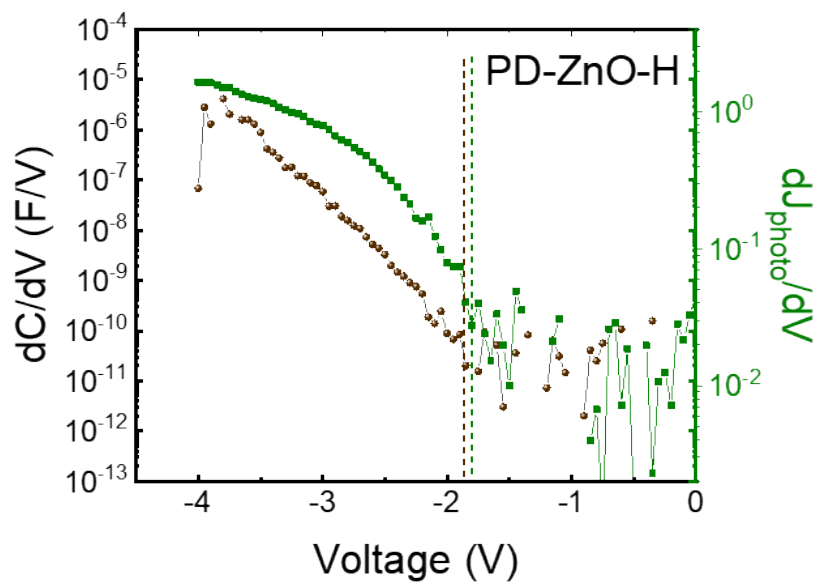
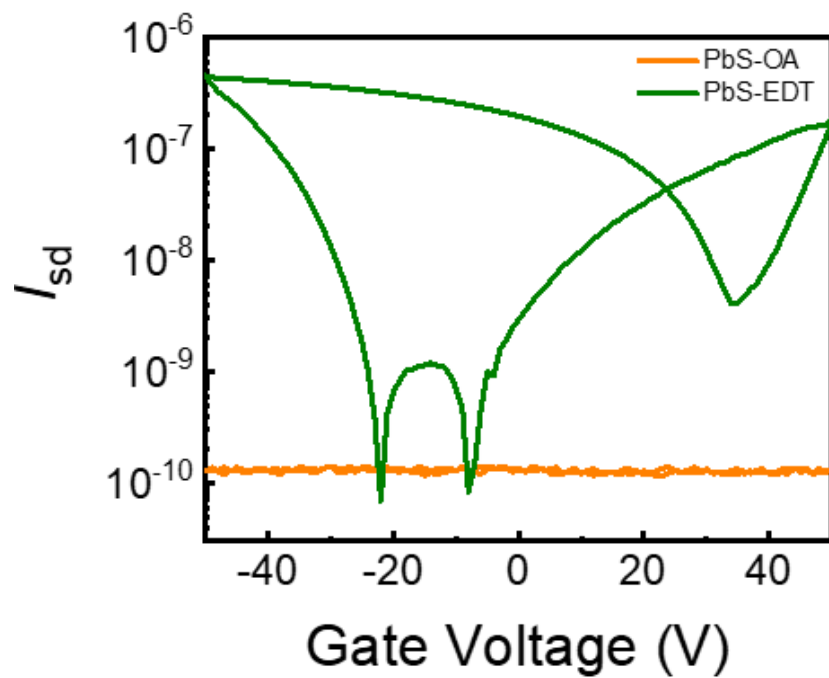


Figure S3. The source-drain current ( $I_{DS}$ ) vs gate voltage ( $V_G$ ) curve of the ZnO thin film-based FET transistor (A) before, after (B) 1 h, and (C) after 2 h of humidity treatment. (D) The calculated electron mobility before and after 1 and 2 h of humidity treatment. (E) Current versus voltage curves of PbS-QPD fabricated using a ZnO layer humidity treated for 2 h. (A rectification ratio between + 0.5 V and - 0.5 V  $\cong 1$ , indicating negligible built-in potential in PbS-QPD.



**Figure S4.**  $dC/dV$ - and  $dJ_{photo}/dV$ - $V$  curves of PD with ZnO-Hydrated.



**Figure S5.** Transfer curves of PbS-EDT and PbS-OA-based FET transistors.

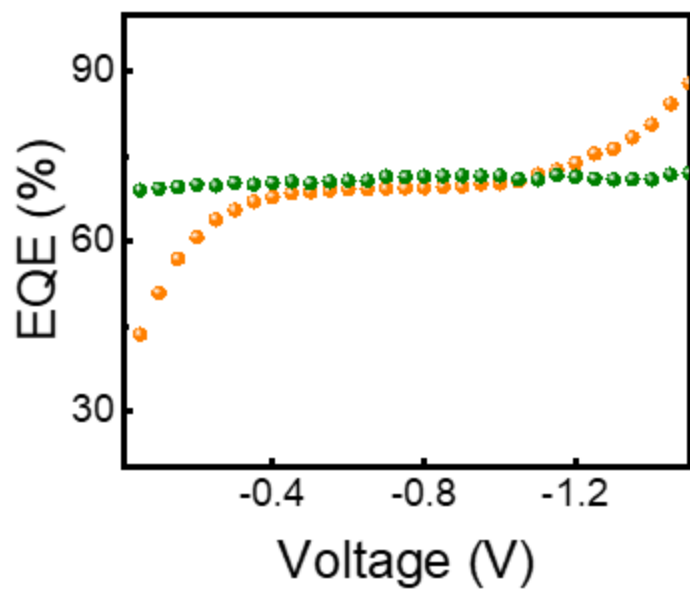


**Figure S6.** The EQEs of PD with PbS-EDT (olive) and PD with PbS-OA (30 nm) (orange) calculated from Figure 3B.

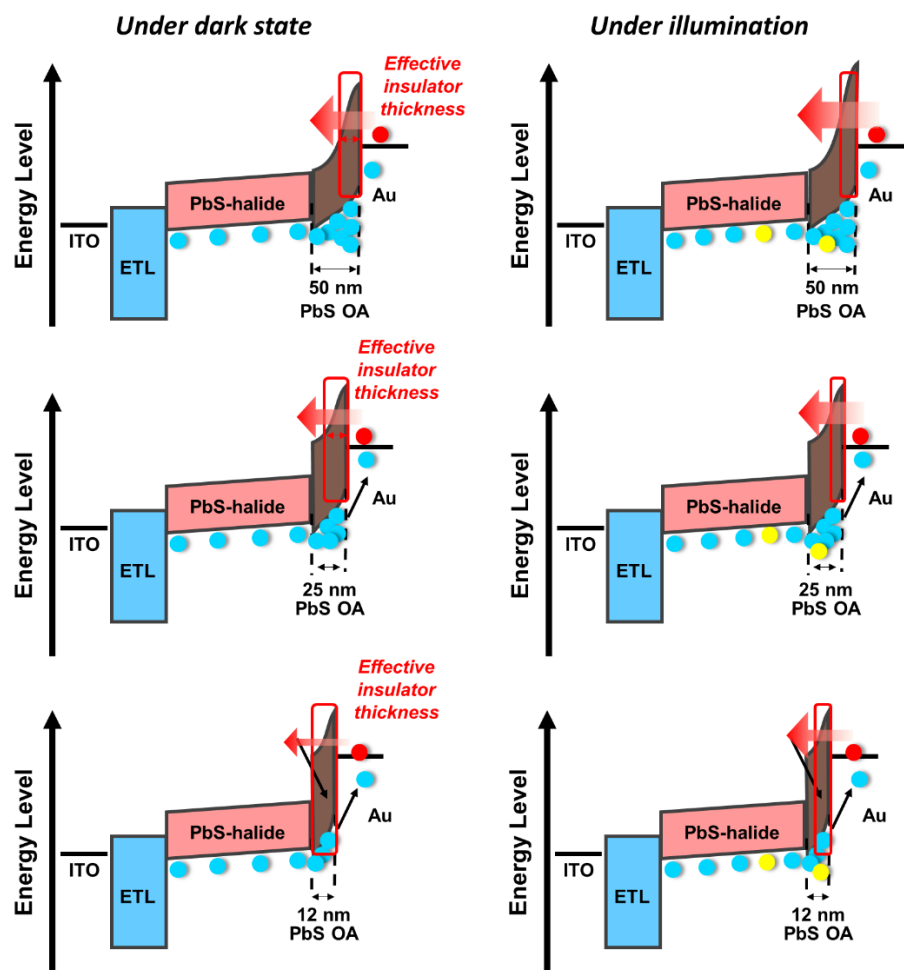


**Figure S7.** Schematic of the mechanism of HTL assisting charge accumulation with different thicknesses of PbS-OA.



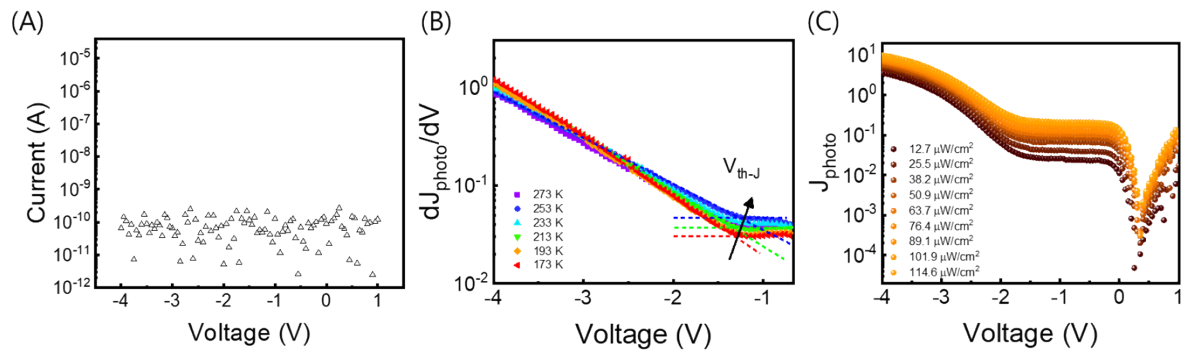


**Figure S8.** (A)  $J$ - $V$  curve of PD with PbS-OA (100 nm) without illumination, (B)  $dJ_{photo}/dV$  versus voltage curves of PD with PbS-OA measured under different temperature, (C)  $J_{photo}$ - $V$  curve of PD with PbS-OA (30 nm) with various light intensity from  $12.7 \mu W cm^{-2}$  to  $114.59 \mu W cm^{-2}$ .

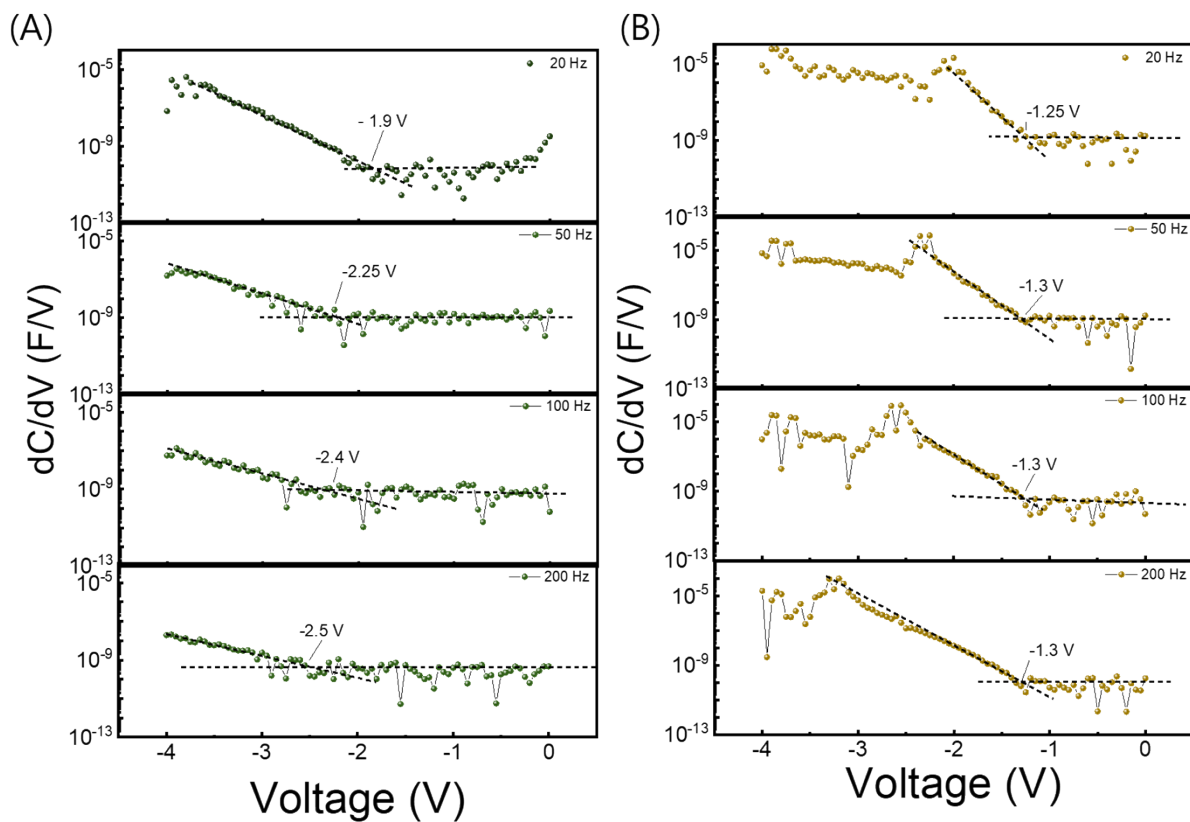


**Figure S9.**  $dC/dV$  versus  $V$  curves of (A) PD with PbS-EDT and (B) PD with PbS-OA measured at 20 Hz, 50 Hz, 100 Hz, and 200 Hz.

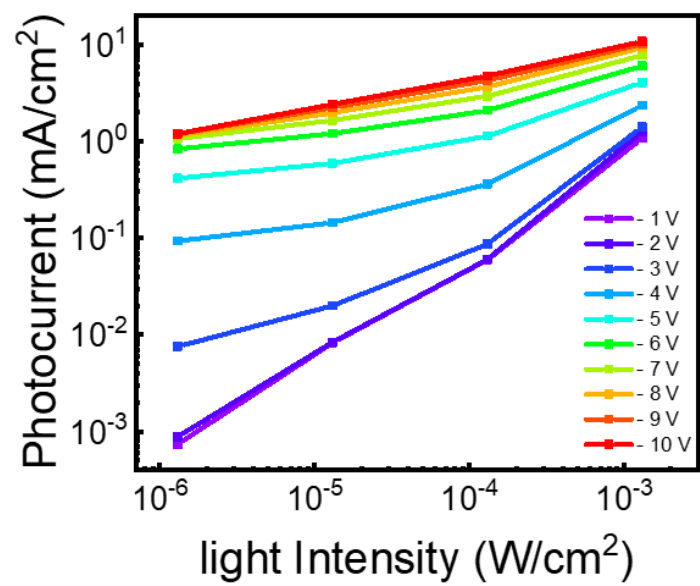


**Figure S10.** Photocurrent density vs light intensity of PM-QPD from – 1 V to – 10 V.

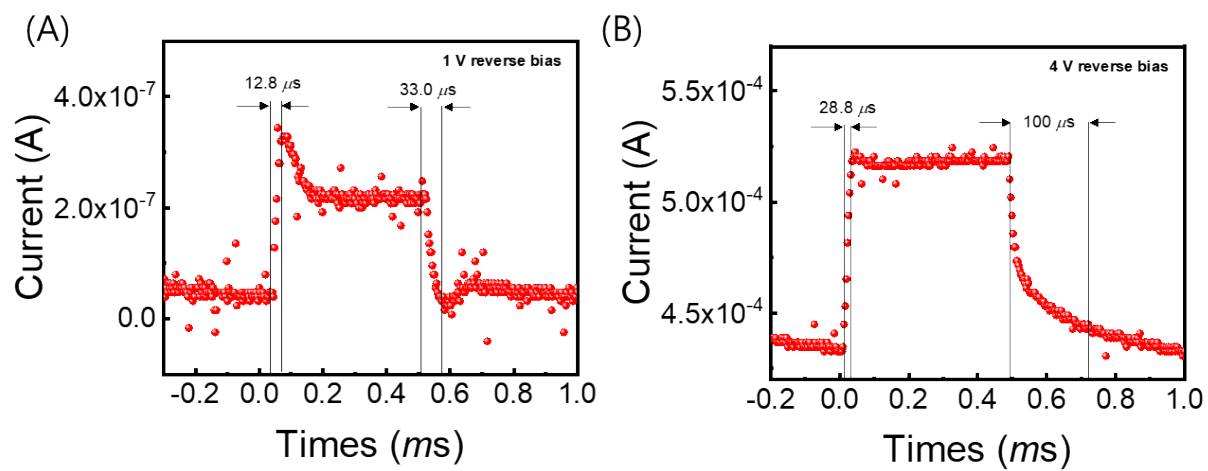


**Figure S11.** Response speed of PM-QPD at (A) – 1 V and (B) – 4 V bias.

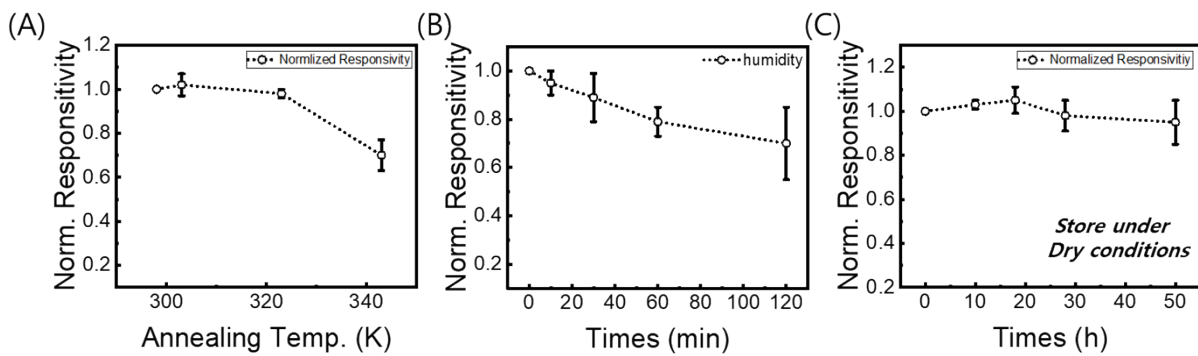


**Figure S12.** The changes in PM-QPD responsivity under (A) different temperatures and long-term storage under (B) high humidity (relative humidity = 70%) and dry (relative humidity < 30%) conditions.

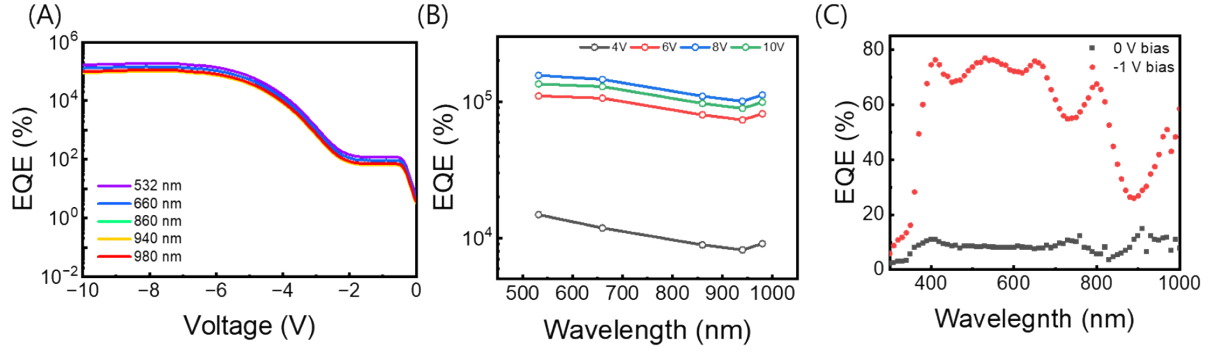


**Figure S13.** (A)  $J$ - $V$  curve of PM-QPD under 532, 660, 860, 940, and 980 nm LED illumination with a light intensity of  $1.3 \mu\text{W cm}^{-2}$  and (B) calculated EQE spectra under 4, 6, 8, and 10 V reverse bias. (C) EQE spectra of PM-QPD under 0 V and -1 V reverse bias.

Device structure	EQE @ voltage	Reference
ITO/ZnO/P3HT/DRCN5T/Al	10 <sup>3</sup> % @ -10 V	[1]
ITO/PEIE/P3HT:PCBM/PEDOT:PSS/Ag	10 <sup>4</sup> % @ -20V	[2]
ITO/ZnPc/C <sub>60</sub> /HATNA-Cl <sub>6</sub> /Al	10 <sup>3</sup> % @ -10 V	[3]
ITO/ZnO:HAc/PbS-halide/PbS-MPA/Au	10 <sup>3</sup> % @ -1 V	[4]
ITO/ZnO/PbS-halide/TAPC/MoO <sub>3</sub> /Ag	10 <sup>4</sup> % @ -10 V	[5]
ITO/ZnO/PbS-halide/PbS-OA/Au	10 <sup>5</sup> % @ -10 V	This work

Table S1. Device performance of various photomultiplication-type photodiodes.

## **Supporting Information Note 1**

The PL spectra of ZnO-D exhibited two different emission peaks corresponding to a sharp band edge emission at 371.2 nm and an oxygen vacancy originating from the broad emission at 540.4 nm (Figure S1A). After the humidity treatment, a 4.8 nm red-shift of the band edge emission peak and a large quenching of the two peaks were observed. We attributed this red-shift in the PL spectrum to the reduced quantum confinement effect of the ZnO NPs by sintering between the constituent ZnO NPs. The quenching of the two peaks indicates the formation of deep in-gap states that induce nonradiative recombination.



## **Supporting Information Note 2**

In contrast to the common belief that tunneling current decreases as the insulator thickness increases, we observed that when the thickness of PbS-OA becomes thicker from 13 to 50 nm, not only does the value of the threshold voltage decrease but also the current increases in the multiplication voltage regime. This is because tunneling was induced by the charge accumulation layer. Accumulated carriers inside the charge accumulation layer form a strong local-electrical field, resulting in band bending and tunneling (Figure S7); therefore, the tunneling current is proportional to the accumulated charge carriers.

## Reference

- [1] J. Miao, M. Du, Y. Fang and F. Zhang, *Nanoscale*, 2019, 11, 16406–16413.
- [2] Y.-L. Wu, K. Fukuda, T. Yokota, T. Someya, Y. Wu, T. Yokota, T. Someya and K. Fukuda, *Advanced Materials*, 2019, 31, 1903687.
- [3] J. Kublitski, A. Fischer, S. Xing, L. Baisinger, E. Bittrich, D. Spoltore, J. Benduhn, K. Vandewal and K. Leo, *Nature Communications* 2021 12:1, 2021, 12, 1–9.
- [4] K. Xu, L. Ke, H. Dou, R. Xu, W. Zhou, Q. Wei, X. Sun, H. Wang, H. Wu, L. Li, J. Xue, B. Chen, T. C. Weng, L. Zheng, Y. Yu and Z. Ning, *ACS Appl Mater Interfaces*, 2022, 14, 14783–14790.
- [5] J. W. Lee, D. Y. Kim and F. So, *Adv Funct Mater*, 2015, 25, 1233–1238.